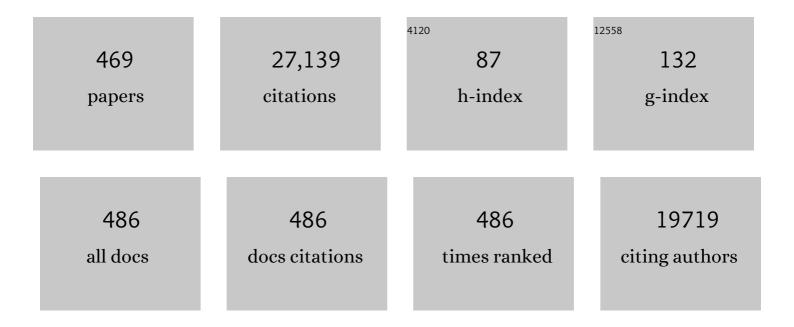
List of Publications by Year in descending order

Source: https://exaly.com/author-pdf/1344630/publications.pdf Version: 2024-02-01



#	Article	IF	CITATIONS
1	A review on the recent progress, challenges and perspective of layered double hydroxides as promising photocatalysts. Journal of Materials Chemistry A, 2016, 4, 10744-10766.	5.2	583
2	Visible light-driven novel g-C ₃ N ₄ /NiFe-LDH composite photocatalyst with enhanced photocatalytic activity towards water oxidation and reduction reaction. Journal of Materials Chemistry A, 2015, 3, 18622-18635.	5.2	500
3	Facile synthesis of highly active g-C3N4 for efficient hydrogen production under visible light. Journal of Materials Chemistry A, 2013, 1, 7816.	5.2	431
4	Adsorption of phosphate by layered double hydroxides in aqueous solutions. Applied Clay Science, 2006, 32, 252-260.	2.6	416
5	Recent advances in anion doped g-C3N4 photocatalysts: A review. Carbon, 2021, 172, 682-711.	5.4	339
6	Fabrication of nanocrystalline LaFeO3: An efficient sol–gel auto-combustion assisted visible light responsive photocatalyst for water decomposition. International Journal of Hydrogen Energy, 2010, 35, 12161-12168.	3.8	309
7	Carbonate intercalated Zn/Fe layered double hydroxide: A novel photocatalyst for the enhanced photo degradation of azo dyes. Chemical Engineering Journal, 2012, 179, 131-139.	6.6	306
8	Fabrication of α-Fe ₂ O ₃ Nanorod/RGO Composite: A Novel Hybrid Photocatalyst for Phenol Degradation. ACS Applied Materials & Interfaces, 2013, 5, 9101-9110.	4.0	291
9	Enhanced Photocatalytic Activities of RhB Degradation and H ₂ Evolution from in Situ Formation of the Electrostatic Heterostructure MoS ₂ /NiFe LDH Nanocomposite through the Z-Scheme Mechanism via p–n Heterojunctions. ACS Applied Materials & Interfaces, 2019, 11, 20923-20942.	4.0	263
10	Physicochemical characterization and adsorption behavior of calcined Zn/Al hydrotalcite-like compound (HTlc) towards removal of fluoride from aqueous solution. Journal of Colloid and Interface Science, 2003, 261, 213-220.	5.0	257
11	An overview of the structural, textural and morphological modulations of g-C ₃ N ₄ towards photocatalytic hydrogen production. RSC Advances, 2016, 6, 46929-46951.	1.7	255
12	Green Synthesis of Fe ₃ O ₄ /RGO Nanocomposite with Enhanced Photocatalytic Performance for Cr(VI) Reduction, Phenol Degradation, and Antibacterial Activity. ACS Sustainable Chemistry and Engineering, 2017, 5, 10551-10562.	3.2	235
13	A review on TiO2/g-C3N4 visible-light- responsive photocatalysts for sustainable energy generation and environmental remediation. Journal of Environmental Chemical Engineering, 2020, 8, 103896.	3.3	227
14	Fabrication of Novel p-BiOI/n-ZnTiO ₃ Heterojunction for Degradation of Rhodamine 6G under Visible Light Irradiation. Inorganic Chemistry, 2013, 52, 6390-6401.	1.9	226
15	An overview on Ag modified g-C3N4 based nanostructured materials for energy and environmental applications. Renewable and Sustainable Energy Reviews, 2018, 82, 1297-1312.	8.2	211
16	Facile Synthesis of Au/gâ€C ₃ N ₄ Nanocomposites: An Inorganic/Organic Hybrid Plasmonic Photocatalyst with Enhanced Hydrogen Gas Evolution Under Visibleâ€Light Irradiation. ChemCatChem, 2014, 6, 1453-1462.	1.8	208
17	Synthesis and characterization of nano-sized porous gamma-alumina by control precipitation method. Materials Chemistry and Physics, 2009, 113, 244-248.	2.0	202
18	An overview of the modification of g-C ₃ N ₄ with high carbon containing materials for photocatalytic applications. Inorganic Chemistry Frontiers, 2016, 3, 336-347.	3.0	201

#	Article	IF	CITATIONS
19	Facile fabrication of α-FeOOH nanorod/RGO composite: a robust photocatalyst for reduction of Cr(<scp>vi</scp>) under visible light irradiation. Journal of Materials Chemistry A, 2014, 2, 10300-10312.	5.2	199
20	Visible light induced photocatalytic activity of rare earth titania nanocomposites. Journal of Molecular Catalysis A, 2008, 287, 151-158.	4.8	198
21	Dynamics of Charge-Transfer Behavior in a Plasmon-Induced Quasi-Type-II p–n/n–n Dual Heterojunction in Ag@Ag ₃ PO ₄ /g-C ₃ N ₄ /NiFe LDH Nanocomposites for Photocatalytic Cr(VI) Reduction and Phenol Oxidation. ACS Omega, 2018, 3, 7324-7343.	1.6	197
22	Highly efficient charge transfer through a double Z-scheme mechanism by a Cu-promoted MoO ₃ /g-C ₃ N ₄ hybrid nanocomposite with superior electrochemical and photocatalytic performance. Nanoscale, 2018, 10, 5950-5964.	2.8	195
23	Recent advances in phase, size, and morphology-oriented nanostructured nickel phosphide for overall water splitting. Journal of Materials Chemistry A, 2020, 8, 19196-19245.	5.2	194
24	Design and development of a visible light harvesting Ni–Zn/Cr–CO32â^ LDH system for hydrogen evolution. Journal of Materials Chemistry A, 2013, 1, 4236.	5.2	190
25	Fabrication, Growth Mechanism, and Characterization of α-Fe ₂ O ₃ Nanorods. ACS Applied Materials & Interfaces, 2011, 3, 317-323.	4.0	174
26	Deciphering Z-scheme Charge Transfer Dynamics in Heterostructure NiFe-LDH/N-rGO/g-C3N4 Nanocomposite for Photocatalytic Pollutant Removal and Water Splitting Reactions. Scientific Reports, 2019, 9, 2458.	1.6	173
27	Facile Synthesis of N- and S-Incorporated Nanocrystalline TiO ₂ and Direct Solar-Light-Driven Photocatalytic Activity. Journal of Physical Chemistry C, 2010, 114, 19473-19482.	1.5	166
28	Enhanced photo catalytic reduction of Cr (VI) over polymer-sensitized g-C3N4/ZnFe2O4 and its synergism with phenol oxidation under visible light irradiation. Catalysis Today, 2018, 315, 52-66.	2.2	166
29	Fabrication of a Co(OH) ₂ /ZnCr LDH "p–n―Heterojunction Photocatalyst with Enhanced Separation of Charge Carriers for Efficient Visible-Light-Driven H ₂ and O ₂ Evolution. Inorganic Chemistry, 2018, 57, 3840-3854.	1.9	162
30	Synergistic Effects of Boron and Sulfur Co-doping into Graphitic Carbon Nitride Framework for Enhanced Photocatalytic Activity in Visible Light Driven Hydrogen Generation. ACS Applied Energy Materials, 2018, 1, 5936-5947.	2.5	162
31	Amine functionalized MCM-41: An active and reusable catalyst for Knoevenagel condensation reaction. Journal of Molecular Catalysis A, 2009, 310, 93-100.	4.8	157
32	Enhanced photocatalytic activities of polypyrrole sensitized zinc ferrite/graphitic carbon nitride n-n heterojunction towards ciprofloxacin degradation, hydrogen evolution and antibacterial studies. Journal of Colloid and Interface Science, 2020, 561, 551-567.	5.0	156
33	Molybdate/Tungstate Intercalated Oxo-Bridged Zn/Y LDH for Solar Light Induced Photodegradation of Organic Pollutants. Journal of Physical Chemistry C, 2012, 116, 13063-13070.	1.5	155
34	Incorporation of Fe3+ into Mg/Al layered double hydroxide framework: effects on textural properties and photocatalytic activity for H2 generation. Journal of Materials Chemistry, 2012, 22, 7350.	6.7	155
35	Photocatalytic reduction of hexavalent chromium in aqueous solution over sulphate modified titania. Journal of Photochemistry and Photobiology A: Chemistry, 2005, 170, 189-194.	2.0	152
36	Resurrection of boron nitride in p-n type-II boron nitride/B-doped-g-C3N4 nanocomposite during solid-state Z-scheme charge transfer path for the degradation of tetracycline hydrochloride. Journal of Colloid and Interface Science, 2020, 566, 211-223.	5.0	152

#	Article	IF	CITATIONS
37	Studies on MnO2—I. Chemical composition, microstructure and other characteristics of some synthetic MnO2 of various crystalline modifications. Electrochimica Acta, 1981, 26, 435-443.	2.6	151
38	Effect of Co ²⁺ Substitution in the Framework of Carbonate Intercalated Cu/Cr LDH on Structural, Electronic, Optical, and Photocatalytic Properties. Journal of Physical Chemistry C, 2012, 116, 22417-22424.	1.5	150
39	Modification of BiOI Microplates with CdS QDs for Enhancing Stability, Optical Property, Electronic Behavior toward Rhodamine B Decolorization, and Photocatalytic Hydrogen Evolution. Journal of Physical Chemistry C, 2017, 121, 4834-4849.	1.5	150
40	An overview on visible light responsive metal oxide based photocatalysts for hydrogen energy production. RSC Advances, 2015, 5, 61535-61553.	1.7	148
41	Physico-chemical characterization and photocatalytic activity of zinc oxide prepared by various methods. Journal of Colloid and Interface Science, 2006, 298, 787-793.	5.0	139
42	A facile in situ approach to fabricate N,S-TiO ₂ /g-C ₃ N ₄ nanocomposite with excellent activity for visible light induced water splitting for hydrogen evolution. Physical Chemistry Chemical Physics, 2015, 17, 8070-8077.	1.3	138
43	Effects of Co, Ni, Cu, and Zn on Photophysical and Photocatalytic Properties of Carbonate Intercalated M ^{II} /Cr LDHs for Enhanced Photodegradation of Methyl Orange. Industrial & Engineering Chemistry Research, 2014, 53, 3834-3841.	1.8	136
44	Studies on MnO2—III. The kinetics and the mechanism for the catalytic decomposition of H2O2 over different crystalline modifications of MnO2. Electrochimica Acta, 1981, 26, 1157-1167.	2.6	129
45	Construction of a Z-Scheme Dictated WO _{3–<i>X</i>} /Ag/ZnCr LDH Synergistically Visible Light-Induced Photocatalyst towards Tetracycline Degradation and H ₂ Evolution. ACS Omega, 2019, 4, 14721-14741.	1.6	129
46	HPW-Anchored UiO-66 Metal–Organic Framework: A Promising Photocatalyst Effective toward Tetracycline Hydrochloride Degradation and H ₂ Evolution via Z-Scheme Charge Dynamics. Inorganic Chemistry, 2019, 58, 4921-4934.	1.9	129
47	Zn–Cr layered double hydroxide: Visible light responsive photocatalyst for photocatalytic degradation of organic pollutants. Separation and Purification Technology, 2012, 91, 73-80.	3.9	128
48	Constructing a Novel Surfactant-free MoS ₂ Nanosheet Modified MgIn ₂ S ₄ Marigold Microflower: An Efficient Visible-Light Driven 2D-2D p-n Heterojunction Photocatalyst toward HER and pH Regulated NRR. ACS Sustainable Chemistry and Engineering, 2020, 8, 4848-4862.	3.2	127
49	Fabrication of In2O3 modified ZnO for enhancing stability, optical behaviour, electronic properties and photocatalytic activity for hydrogen production under visible light. Journal of Materials Chemistry A, 2014, 2, 3621.	5.2	125
50	Recent progress in first row transition metal Layered double hydroxide (LDH) based electrocatalysts towards water splitting: A review with insights on synthesis. Coordination Chemistry Reviews, 2022, 469, 214666.	9.5	125
51	Preparation, characterization, and photocatalytic activity of sulfate-modified titania for degradation of methyl orange under visible light. Journal of Colloid and Interface Science, 2008, 318, 231-237.	5.0	124
52	Recent progress in the development of carbonate-intercalated Zn/Cr LDH as a novel photocatalyst for hydrogen evolution aimed at the utilization of solar light. Dalton Transactions, 2012, 41, 1173-1178.	1.6	124
53	Facile Synthesis of CeO ₂ Nanosheets Decorated upon BiOI Microplate: A Surface Oxygen Vacancy Promoted Z-Scheme-Based 2D-2D Nanocomposite Photocatalyst with Enhanced Photocatalytic Activity. Journal of Physical Chemistry C, 2018, 122, 808-819.	1.5	123
54	Coupling of Crumpled-Type Novel MoS ₂ with CeO ₂ Nanoparticles: A Noble-Metal-Free p–n Heterojunction Composite for Visible Light Photocatalytic H ₂ Production. ACS Omega, 2017, 2, 3745-3753.	1.6	121

#	Article	IF	CITATIONS
55	Photocatalytic degradation of phenol under solar radiation using microwave irradiated zinc oxide. Solar Energy, 2006, 80, 1048-1054.	2.9	118
56	The effect of sulfate pre-treatment to improve the deposition of Au-nanoparticles in a gold-modified sulfated g-C ₃ N ₄ plasmonic photocatalyst towards visible light induced water reduction reaction. Physical Chemistry Chemical Physics, 2016, 18, 28502-28514.	1.3	118
57	Fabrication of Hierarchical Two-Dimensional MoS ₂ Nanoflowers Decorated upon Cubic Caln ₂ S ₄ Microflowers: Facile Approach To Construct Novel Metal-Free p–n Heterojunction Semiconductors with Superior Charge Separation Efficiency. Inorganic Chemistry, 2018. 57, 10059-10071.	1.9	117
58	Nanostructured CeO2/MgAl-LDH composite for visible light induced water reduction reaction. International Journal of Hydrogen Energy, 2016, 41, 21166-21180.	3.8	115
59	UiO-66-NH ₂ Metal–Organic Frameworks with Embedded MoS ₂ Nanoflakes for Visible-Light-Mediated H ₂ and O ₂ Evolution. Inorganic Chemistry, 2020, 59, 9824-9837.	1.9	115
60	Methane emission from flooded rice fields under irrigated conditions. Biology and Fertility of Soils, 1994, 18, 245-248.	2.3	113
61	Synergistic ZnFe2O4-carbon allotropes nanocomposite photocatalyst for norfloxacin degradation and Cr (VI) reduction. Journal of Colloid and Interface Science, 2019, 544, 96-111.	5.0	112
62	A type-II interband alignment heterojunction architecture of cobalt titanate integrated UiO-66-NH2: A visible light mediated photocatalytic approach directed towards Norfloxacin degradation and green energy (Hydrogen) evolution. Journal of Colloid and Interface Science, 2020, 568, 89-105.	5.0	112
63	Studies on Ferric Oxide Hydroxides. Journal of Colloid and Interface Science, 1997, 185, 355-362.	5.0	109
64	A mechanistic approach towards the photocatalytic organic transformations over functionalised metal organic frameworks: a review. Catalysis Science and Technology, 2018, 8, 679-696.	2.1	109
65	Facile synthesis of visible light responsive V2O5/N,S–TiO2 composite photocatalyst: enhanced hydrogen production and phenol degradation. Journal of Materials Chemistry, 2012, 22, 10695.	6.7	107
66	Facile synthesis of exfoliated graphitic carbon nitride for photocatalytic degradation of ciprofloxacin under solar irradiation. Journal of Materials Science, 2019, 54, 5726-5742.	1.7	107
67	Quantum dots as enhancer in photocatalytic hydrogen evolution: A review. International Journal of Hydrogen Energy, 2017, 42, 9467-9481.	3.8	104
68	Synthesis of mesoporous TiO2â^'xNx spheres by template free homogeneous co-precipitation method and their photo-catalytic activity under visible light illumination. Journal of Colloid and Interface Science, 2009, 333, 269-276.	5.0	102
69	Cr(VI) remediation from aqueous environment through modified-TiO ₂ -mediated photocatalytic reduction. Beilstein Journal of Nanotechnology, 2018, 9, 1448-1470.	1.5	102
70	One-Pot-Architectured Au-Nanodot-Promoted MoS ₂ /Znln ₂ S ₄ : A Novel p–n Heterojunction Photocatalyst for Enhanced Hydrogen Production and Phenol Degradation. Inorganic Chemistry, 2019, 58, 9941-9955.	1.9	102
71	Plasmon Induced Nano Au Particle Decorated over S,N-Modified TiO ₂ for Exceptional Photocatalytic Hydrogen Evolution under Visible Light. ACS Applied Materials & Interfaces, 2014, 6, 839-846.	4.0	99
72	The enhanced photocatalytic activity of g-C ₃ N ₄ -LaFeO ₃ for the water reduction reaction through a mediator free Z-scheme mechanism. Inorganic Chemistry Frontiers, 2017, 4, 1022-1032.	3.0	99

#	Article	IF	CITATIONS
73	Structural properties and catalytic oxidation of benzene to phenol over CuO-impregnated mesoporous silica. Applied Catalysis A: General, 2007, 321, 101-108.	2.2	98
74	Efficient Photon Conversion via Double Charge Dynamics CeO ₂ –BiFeO ₃ p–n Heterojunction Photocatalyst Promising toward N ₂ Fixation and Phenol–Cr(VI) Detoxification. Inorganic Chemistry, 2020, 59, 3856-3873.	1.9	98
75	Adsorption of toxic metal ion Cr(VI) from aqueous state by TiO2-MCM-41: Equilibrium and kinetic studies. Journal of Hazardous Materials, 2012, 241-242, 395-403.	6.5	96
76	Studies on Mg/Fe Hydrotalcite-Like-Compound (HTlc). Journal of Colloid and Interface Science, 2002, 251, 26-32.	5.0	95
77	Synthesis, characterization, and catalytic activity of phosphomolybdic acid supported on hydrous zirconia. Journal of Colloid and Interface Science, 2006, 300, 237-243.	5.0	95
78	Construction of M-BiVO4/T-BiVO4 isotype heterojunction for enhanced photocatalytic degradation of Norfloxacine and Oxygen evolution reaction. Journal of Colloid and Interface Science, 2019, 554, 278-295.	5.0	95
79	An overview of recent progress on noble metal modified magnetic Fe ₃ O ₄ for photocatalytic pollutant degradation and H ₂ evolution. Catalysis Science and Technology, 2019, 9, 916-941.	2.1	95
80	Fabrication of mesoporous CuO/ZrO 2 -MCM-41 nanocomposites for photocatalytic reduction of Cr(VI). Chemical Engineering Journal, 2017, 316, 1122-1135.	6.6	94
81	Hydrolytically stable citrate capped Fe3O4@UiO-66-NH2 MOF: A hetero-structure composite with enhanced activity towards Cr (VI) adsorption and photocatalytic H2 evolution. Journal of Colloid and Interface Science, 2022, 606, 353-366.	5.0	94
82	Mg/Al hydrotalcites: preparation, characterisation and ketonisation of acetic acid. Journal of Molecular Catalysis A, 2000, 151, 185-192.	4.8	92
83	Facile fabrication of Bi2O3/TiO2-xNx nanocomposites for excellent visible light driven photocatalytic hydrogen evolution. International Journal of Hydrogen Energy, 2011, 36, 2794-2802.	3.8	92
84	Liquid phase catalytic oxidation of benzyl alcohol to benzaldehyde over vanadium phosphate catalyst. Applied Catalysis A: General, 2012, 413-414, 245-253.	2.2	92
85	Facile synthesis of ZnFe2O4@RGO nanocomposites towards photocatalytic ciprofloxacin degradation and H2 energy production. Journal of Colloid and Interface Science, 2019, 556, 667-679.	5.0	92
86	Synergistic effects of plasmon induced Ag@Ag ₃ VO ₄ /ZnCr LDH ternary heterostructures towards visible light responsive O ₂ evolution and phenol oxidation reactions. Inorganic Chemistry Frontiers, 2018, 5, 879-896.	3.0	91
87	Visible-light driven Gd2Ti2O7/GdCrO3 composite for hydrogen evolution. Dalton Transactions, 2011, 40, 12839.	1.6	90
88	Green synthesis of Au/TiO2 for effective dye degradation in aqueous system. Chemical Engineering Journal, 2013, 229, 492-497.	6.6	90
89	Orienting Z scheme charge transfer in graphitic carbon nitride-based systems for photocatalytic energy and environmental applications. Journal of Materials Chemistry A, 2021, 9, 10039-10080.	5.2	90
90	Photocatalytic reduction of hexavalent chromium in aqueous solution over titania pillared zirconium phosphate and titanium phosphate under solar radiation. Journal of Molecular Catalysis A, 2006, 245, 217-224.	4.8	89

#	Article	IF	CITATIONS
91	Amine functionalized K10 montmorillonite: a solid acid–base catalyst for the Knoevenagel condensation reaction. Dalton Transactions, 2013, 42, 5122.	1.6	89
92	A review of harvesting clean fuels from enzymatic CO ₂ reduction. RSC Advances, 2016, 6, 44170-44194.	1.7	87
93	Synthesis, photoelectrochemical properties and solar light-induced photocatalytic activity of bismuth ferrite nanoparticles. Journal of Nanoparticle Research, 2018, 20, 1.	0.8	87
94	A facile method for synthesis of amine-functionalized mesoporous zirconia and its catalytic evaluation in Knoevenagel condensation. Applied Catalysis A: General, 2010, 381, 226-232.	2.2	86
95	MOF derived nano-materials: A recent progress in strategic fabrication, characterization and mechanistic insight towards divergent photocatalytic applications. Coordination Chemistry Reviews, 2022, 456, 214392.	9.5	86
96	Serendipitous Assembly of Mixed Phase BiVO ₄ on B-Doped g-C ₃ N ₄ : An Appropriate p–n Heterojunction for Photocatalytic O ₂ evolution and Cr(VI) reduction. Inorganic Chemistry, 2019, 58, 12480-12491.	1.9	85
97	Superactive NiFe-LDH/graphene nanocomposites as competent catalysts for water splitting reactions. Inorganic Chemistry Frontiers, 2020, 7, 3805-3836.	3.0	85
98	Synthesis of Multifunctional Nanostructured Zinc–Iron Mixed Oxide Photocatalyst by a Simple Solution-Combustion Technique. ACS Applied Materials & Interfaces, 2012, 4, 707-713.	4.0	84
99	Transition metal/metal oxide modified MCM-41 for pollutant degradation and hydrogen energy production: a review. RSC Advances, 2015, 5, 83707-83724.	1.7	84
100	Structural properties and catalytic activity of Mn-MCM-41 mesoporous molecular sieves for single-step amination of benzene to aniline. Applied Catalysis A: General, 2008, 351, 59-67.	2.2	83
101	Enhanced photocatalytic activity of nanostructured Fe doped CeO2 for hydrogen production under visible light irradiation. International Journal of Hydrogen Energy, 2016, 41, 14133-14146.	3.8	83
102	Topotactic Transformation of Solvated MgCr-LDH Nanosheets to Highly Efficient Porous MgO/MgCr ₂ O ₄ Nanocomposite for Photocatalytic H ₂ Evolution. Inorganic Chemistry, 2018, 57, 8646-8661.	1.9	83
103	Preparation, physico-chemical characterization and catalytic activity of sulphated ZrO2–TiO2 mixed oxides. Journal of Molecular Catalysis A, 2002, 189, 271-282.	4.8	81
104	Preparation and characterization of Mg–Al hydrotalcite-like compounds containing cerium. Journal of Colloid and Interface Science, 2006, 301, 569-574.	5.0	81
105	Dramatic activities of vanadate intercalated bismuth doped LDH for solar light photocatalysis. Physical Chemistry Chemical Physics, 2014, 16, 16985-16996.	1.3	81
106	CuO/PbTiO ₃ : A new-fangled p–n junction designed for the efficient absorption of visible light with augmented interfacial charge transfer, photoelectrochemical and photocatalytic activities. Journal of Materials Chemistry A, 2017, 5, 20359-20373.	5.2	81
107	Metal oxide integrated metal organic frameworks (MO@MOF): rational design, fabrication strategy, characterization and emerging photocatalytic applications. Inorganic Chemistry Frontiers, 2021, 8, 1619-1636.	3.0	81
108	CdS QDs-Decorated Self-Doped Î ³ -Bi ₂ MoO ₆ : A Sustainable and Versatile Photocatalyst toward Photoreduction of Cr(VI) and Degradation of Phenol. ACS Omega, 2017, 2, 9040-9056.	1.6	79

#	Article	IF	CITATIONS
109	n-La ₂ Ti ₂ O ₇ /p-LaCrO ₃ : a novel heterojunction based composite photocatalyst with enhanced photoactivity towards hydrogen production. Journal of Materials Chemistry A, 2014, 2, 18405-18412.	5.2	78
110	Facile synthesis of ZnFe ₂ O ₄ photocatalysts for decolourization of organic dyes under solar irradiation. Beilstein Journal of Nanotechnology, 2018, 9, 436-446.	1.5	77
111	Facile construction of a novel NiFe ₂ O ₄ @P-doped g-C ₃ N ₄ nanocomposite with enhanced visible-light-driven photocatalytic activity. Nanoscale Advances, 2019, 1, 1864-1879.	2.2	77
112	Double charge carrier mechanism through 2D/2D interface-assisted ultrafast water reduction and antibiotic degradation over architectural S,P co-doped g-C ₃ N ₄ /ZnCr LDH photocatalyst. Inorganic Chemistry Frontiers, 2020, 7, 3695-3717.	3.0	77
113	Pyrochlore Ce ₂ Zr ₂ O ₇ decorated over rGO: a photocatalyst that proves to be efficient towards the reduction of 4-nitrophenol and degradation of ciprofloxacin under visible light. Physical Chemistry Chemical Physics, 2018, 20, 9872-9885.	1.3	76
114	Calcined Mg–Fe–CO3 LDH as an adsorbent for the removal of selenite. Journal of Colloid and Interface Science, 2007, 316, 216-223.	5.0	75
115	Synthesis, characterisation and catalytic evaluation of iron–manganese mixed oxide pillared clay for VOC decomposition reaction. Applied Catalysis B: Environmental, 2008, 79, 279-285.	10.8	75
116	Manganese containing MCM-41: Synthesis, characterization and catalytic activity in the oxidation of ethylbenzene. Journal of Molecular Catalysis A, 2009, 306, 54-61.	4.8	75
117	The fabrication of Au/Pd plasmonic alloys on UiO-66-NH ₂ : an efficient visible light-induced photocatalyst towards the Suzuki Miyaura coupling reaction under ambient conditions. Catalysis Science and Technology, 2019, 9, 6585-6597.	2.1	75
118	Recent progress on strategies for the preparation of 2D/2D MXene/g-C ₃ N ₄ nanocomposites for photocatalytic energy and environmental applications. Catalysis Science and Technology, 2021, 11, 1222-1248.	2.1	75
119	Enhanced visible light harnessing and oxygen vacancy promoted N, S co-doped CeO ₂ nanoparticle: a challenging photocatalyst for Cr(<scp>vi</scp>) reduction. Catalysis Science and Technology, 2017, 7, 2772-2781.	2.1	74
120	Catalytic ketonisation of acetic acid over modified zirconia. Journal of Molecular Catalysis A, 1999, 139, 73-80.	4.8	73
121	Fabrication of a Au-loaded CaFe ₂ O ₄ /CoAl LDH p–n junction based architecture with stoichiometric H ₂ & O ₂ generation and Cr(<scp>vi</scp>) reduction under visible light. Inorganic Chemistry Frontiers, 2019, 6, 94-109.	3.0	73
122	Copperphthalocyanine immobilized Zn/Al LDH as photocatalyst under solar radiation for decolorization of methylene blue. Journal of Molecular Catalysis A, 2007, 267, 202-208.	4.8	72
123	Silicotungstic acid supported zirconia: An effective catalyst for esterification reaction. Journal of Molecular Catalysis A, 2007, 275, 77-83.	4.8	72
124	Copper and Nickel Modified MCM-41 An Efficient Catalyst for Hydrodehalogenation of Chlorobenzene at Room Temperature. Industrial & Engineering Chemistry Research, 2011, 50, 2839-2849.	1.8	72
125	Efficient hydrogen production by composite photocatalyst CdS–ZnS/Zirconium–titanium phosphate (ZTP) under visible light illumination. International Journal of Hydrogen Energy, 2011, 36, 13452-13460.	3.8	72
126	Bimetallic co-effect of Au-Pd alloyed nanoparticles on mesoporous silica modified g-C3N4 for single and simultaneous photocatalytic oxidation of phenol and reduction of hexavalent chromium. Journal of Colloid and Interface Science, 2020, 560, 519-535.	5.0	72

#	Article	IF	CITATIONS
127	Gold Promoted S,Nâ^'Doped TiO ₂ : An Efficient Catalyst for CO Adsorption and Oxidation. Environmental Science & Technology, 2010, 44, 4155-4160.	4.6	71
128	A novel approach towards solvent-free epoxidation of cyclohexene by Ti(IV)–Schiff base complex-intercalated LDH using H2O2 as oxidant. Journal of Catalysis, 2010, 276, 161-169.	3.1	70
129	Adsorption of Copper(II) on NH ₂ -MCM-41 and Its Application for Epoxidation of Styrene. Industrial & Engineering Chemistry Research, 2012, 51, 2235-2246.	1.8	70
130	Montmorillonite supported metal nanoparticles: an update on syntheses and applications. RSC Advances, 2013, 3, 13583.	1.7	70
131	Methane budget from paddy fields in India. Chemosphere, 1996, 33, 737-757.	4.2	69
132	Heteropoly acid intercalated Zn/Al HTlc as efficient catalyst for esterification of acetic acid using n-butanol. Journal of Molecular Catalysis A, 2007, 264, 248-254.	4.8	69
133	Phosphide protected FeS ₂ anchored oxygen defect oriented CeO ₂ NS based ternary hybrid for electrocatalytic and photocatalytic N ₂ reduction to NH ₃ . Journal of Materials Chemistry A, 2019, 7, 9145-9153.	5.2	69
134	Mixed-Valence Bimetallic Ce/Zr MOF-Based Nanoarchitecture: A Visible-Light-Active Photocatalyst for Ciprofloxacin Degradation and Hydrogen Evolution. Langmuir, 2022, 38, 1766-1780.	1.6	69
135	An energy band compactable B-rGO/PbTiO ₃ p–n junction: a highly dynamic and durable photocatalyst for enhanced photocatalytic H ₂ evolution. Nanoscale, 2019, 11, 22328-22342.	2.8	68
136	Adsorption of hexavalent chromium on manganese nodule leached residue obtained from NH3–SO2 leaching. Journal of Colloid and Interface Science, 2006, 297, 419-425.	5.0	67
137	Rational design of light induced self healed Fe based oxygen vacancy rich CeO ₂ (CeO ₂ NS–FeOOH/Fe ₂ O ₃) nanostructure materials for photocatalytic water oxidation and Cr(<scp>vi</scp>) reduction. Journal of Materials Chemistry A, 2018, 6, 11377-11389.	5.2	66
138	Novel Magnetic Retrievable Visible-Light-Driven Ternary Fe ₃ O ₄ @NiFe ₂ O ₄ /Phosphorus-Doped g-C ₃ N ₄ Nanocomposite Photocatalyst with Significantly Enhanced Activity through a Double-Z-Scheme System. Inorganic Chemistry, 2020, 59, 4255-4272.	1.9	66
139	Physico-chemical characterisation and photocatalytic activity of nanosized SO42â^'/TiO2 towards degradation of 4-nitrophenol. Journal of Molecular Catalysis A, 2003, 198, 277-287.	4.8	65
140	Synthesis and characterization of a Fe(III)-Schiff base complex in a Zn-Al LDH host for cyclohexane oxidation. Journal of Molecular Catalysis A, 2010, 329, 7-12.	4.8	65
141	Fabrication of S, N co-doped α-Fe2O3 nanostructures: effect of doping, OH radical formation, surface area, [110] plane and particle size on the photocatalytic activity. RSC Advances, 2013, 3, 7912.	1.7	65
142	Amine functionalized MCM-41 as a green, efficient, and heterogeneous catalyst for the regioselective synthesis of 5-aryl-2-oxazolidinones, from CO2 and aziridines. Applied Catalysis A: General, 2014, 469, 340-349.	2.2	65
143	A multi-functionalized montmorillonite for co-operative catalysis in one-pot Henry reaction and water pollution remediation. Journal of Materials Chemistry A, 2014, 2, 7526.	5.2	64
144	CdS QDs modified BiOI/Bi2MoO6 nanocomposite for degradation of quinolone and tetracycline types of antibiotics towards environmental remediation. Separation and Purification Technology, 2020, 253, 117523.	3.9	64

#	Article	IF	CITATIONS
145	Quick photo-Fenton degradation of phenolic compounds by Cu/Al ₂ O ₃ –MCM-41 under visible light irradiation: small particle size, stabilization of copper, easy reducibility of Cu and visible light active material. Dalton Transactions, 2013, 42, 558-566.	1.6	63
146	Visible Light Active Single-Crystal Nanorod/Needle-like α-MnO ₂ @RGO Nanocomposites for Efficient Photoreduction of Cr(VI). Journal of Physical Chemistry C, 2017, 121, 6039-6049.	1.5	63
147	ZnCr ₂ O ₄ @ZnO/g ₃ N ₄ : A Tripleâ€Junction Nanostructured Material for Effective Hydrogen and Oxygen Evolution under Visible Light. Energy Technology, 2017, 5, 1687-1701.	1.8	63
148	A comparative study on adsorption and photocatalytic dye degradation under visible light irradiation by mesoporous MnO 2 modified MCM-41 nanocomposite. Microporous and Mesoporous Materials, 2016, 226, 229-242.	2.2	62
149	A Kinetic, Thermodynamic, and Mechanistic Approach toward Adsorption of Methylene Blue over Water-Washed Manganese Nodule Leached Residues. Industrial & Engineering Chemistry Research, 2011, 50, 843-848.	1.8	61
150	Facile fabrication of Bi2O3/Bi–NaTaO3 photocatalysts for hydrogen generation under visible light irradiation. RSC Advances, 2012, 2, 9423.	1.7	61
151	Highly active Pd nanoparticles dispersed on amine functionalized layered double hydroxide for Suzuki coupling reaction. Dalton Transactions, 2011, 40, 7130.	1.6	60
152	Influence of the nature and concentration of precursor metal ions in the brucite layer of LDHs for phosphate adsorption $\hat{a} \in $ a review. RSC Advances, 2013, 3, 23865.	1.7	60
153	Cu@CuO promoted g-C ₃ N ₄ /MCM-41: an efficient photocatalyst with tunable valence transition for visible light induced hydrogen generation. RSC Advances, 2016, 6, 112602-112613.	1.7	60
154	Constructive Interfacial Charge Carrier Separation of a p-CaFe ₂ O ₄ @n-ZnFe ₂ O ₄ Heterojunction Architect Photocatalyst toward Photodegradation of Antibiotics. Inorganic Chemistry, 2019, 58, 16592-16608.	1.9	60
155	Exfoliated Boron Nitride (e-BN) Tailored Exfoliated Graphitic Carbon Nitride (e-CN): An Improved Visible Light Mediated Photocatalytic Approach towards TCH Degradation and H ₂ Evolution. Inorganic Chemistry, 2021, 60, 5021-5033.	1.9	60
156	Facile fabrication of Cd(OH)3 nanorod/RGO composite: Synthesis, characterisation and photocatalytic reduction of Cr(VI). Chemical Engineering Journal, 2014, 255, 78-88.	6.6	59
157	Fe/meso-Al ₂ O ₃ : An Efficient Photo-Fenton Catalyst for the Adsorptive Degradation of Phenol. Industrial & Engineering Chemistry Research, 2010, 49, 8310-8318.	1.8	58
158	Pd(0) Nanoparticles Supported Organofunctionalized Clay Driving C–C Coupling Reactions under Benign Conditions through a Pd(0)/Pd(II) Redox Interplay. Journal of Physical Chemistry C, 2014, 118, 1640-1651.	1.5	58
159	A bimetallic Au–Ag nanoalloy mounted LDH/RGO nanocomposite: a promising catalyst effective towards a coupled system for the photoredox reactions converting benzyl alcohol to benzaldehyde and nitrobenzene to aniline under visible light. Journal of Materials Chemistry A, 2019, 7, 7614-7627.	5.2	58
160	A comparative study on textural characterization: cation-exchange and sorption properties of crystalline α-zirconium(IV), tin(IV), and titanium(IV) phosphates. Journal of Colloid and Interface Science, 2004, 270, 436-445.	5.0	56
161	A plasmonic AuPd bimetallic nanoalloy decorated over a GO/LDH hybrid nanocomposite <i>via</i> a green synthesis route for robust Suzuki coupling reactions: a paradigm shift towards a sustainable future. Catalysis Science and Technology, 2019, 9, 4678-4692.	2.1	56
162	Facile synthesis of nano-structured magnetite in presence of natural surfactant for enhanced photocatalytic activity for water decomposition and Cr (VI) reduction. Chemical Engineering Journal, 2016. 299. 227-235.	6.6	55

#	Article	IF	CITATIONS
163	Sulfate-Anchored Hierarchical Meso–Macroporous N-doped TiO ₂ : A Novel Photocatalyst for Visible Light H ₂ Evolution. ACS Sustainable Chemistry and Engineering, 2014, 2, 1429-1438.	3.2	54
164	Kinetics, Isotherm, and Thermodynamic Study for Ultrafast Adsorption of Azo Dye by an Efficient Sorbent: Ternary Mg/(Al + Fe) Layered Double Hydroxides. ACS Omega, 2018, 3, 2532-2545.	1.6	54
165	Visible light driven LaFeO3 nano sphere/RGO composite photocatalysts for efficient water decomposition reaction. Catalysis Today, 2020, 353, 220-231.	2.2	54
166	Magnetite modified amino group based polymer nanocomposites towards efficient adsorptive detoxification of aqueous Cr (VI): A review. Journal of Molecular Liquids, 2021, 337, 116487.	2.3	54
167	Facile fabrication of hierarchical N-doped GaZn mixed oxides for water splitting reactions. Journal of Materials Chemistry, 2010, 20, 7144.	6.7	53
168	Growth of macroporous TiO ₂ on B-doped g-C ₃ N ₄ nanosheets: a Z-scheme photocatalyst for H ₂ O ₂ production and phenol oxidation under visible light. Inorganic Chemistry Frontiers, 2021, 8, 1489-1499.	3.0	53
169	A review on vertical and lateral heterostructures of semiconducting 2D-MoS ₂ with other 2D materials: a feasible perspective for energy conversion. Nanoscale, 2021, 13, 9908-9944.	2.8	53
170	Development of MgIn ₂ S ₄ Microflower-Embedded Exfoliated B-Doped g-C ₃ N ₄ Nanosheets: p–n Heterojunction Photocatalysts toward Photocatalytic Water Reduction and H ₂ O ₂ Production under Visible-Light Irradiation. ACS Applied Energy Materials, 2022, 5, 2838-2852.	2.5	53
171	Cation Exchange and Sorption Properties of Crystalline α-Titanium(IV) Phosphate. Journal of Colloid and Interface Science, 2002, 248, 221-230.	5.0	52
172	Green synthesis of fibrous hierarchical meso-macroporous N doped TiO2 nanophotocatalyst with enhanced photocatalytic H2 production. International Journal of Hydrogen Energy, 2013, 38, 3545-3553.	3.8	52
173	A review of solar and visible light active oxo-bridged materials for energy and environment. Catalysis Science and Technology, 2017, 7, 2153-2164.	2.1	52
174	Architecture of Biperovskite-Based LaCrO ₃ /PbTiO ₃ p–n Heterojunction with a Strong Interface for Enhanced Charge Anti-recombination Process and Visible Light-Induced Photocatalytic Reactions. Inorganic Chemistry, 2018, 57, 15133-15148.	1.9	52
175	Construction of Isoenergetic Band Alignment between CdS QDs and CaFe ₂ O ₄ @ZnFe ₂ O ₄ Heterojunction: A Promising Ternary Hybrid toward Norfloxacin Degradation and H ₂ Energy Production. Journal of Physical Chemistry C. 2019. 123. 17112-17126.	1.5	52
176	Solar-light induced photodegradation of organic pollutants over CdS-pillared zirconium–titanium phosphate (ZTP). Journal of Molecular Catalysis A, 2011, 349, 36-41.	4.8	51
177	Recent Progress in LDH@Graphene and Analogous Heterostructures for Highly Active and Stable Photocatalytic and Photoelectrochemical Water Splitting. Chemistry - an Asian Journal, 2021, 16, 2211-2248.	1.7	51
178	A review on visible light driven spinel ferrite-g-C3N4 photocatalytic systems with enhanced solar light utilization. Journal of Molecular Liquids, 2022, 357, 119105.	2.3	51
179	Facile Fabrication of S-TiO ₂ /l͡²-SiC Nanocomposite Photocatalyst for Hydrogen Evolution under Visible Light Irradiation. ACS Sustainable Chemistry and Engineering, 2015, 3, 245-253.	3.2	50
180	Biomimetic synthesis, characterization and mechanism of formation of stable silver nanoparticles using Averrhoa carambola L. leaf extract. Materials Letters, 2015, 160, 566-571.	1.3	50

#	Article	IF	CITATIONS
181	Controlled Synthesis of CeO ₂ NS-Au-CdSQDs Ternary Nanoheterostructure: A Promising Visible Light Responsive Photocatalyst for H ₂ Evolution. Inorganic Chemistry, 2017, 56, 12297-12307.	1.9	50
182	Highlights of the characterization techniques on inorganic, organic (COF) and hybrid (MOF) photocatalytic semiconductors. Catalysis Science and Technology, 2021, 11, 392-415.	2.1	50
183	Studies on anion promoted Titania. Journal of Molecular Catalysis A, 2000, 156, 267-274.	4.8	49
184	The effect of dopants on the activity of MoO3/ZSM-5 catalysts for the dehydroaromatisation of methane. Catalysis Today, 2006, 114, 383-387.	2.2	49
185	Transforming inorganic layered montmorillonite into inorganic–organic hybrid materials for various applications: a brief overview. Inorganic Chemistry Frontiers, 2016, 3, 1100-1111.	3.0	49
186	Exfoliated metal free homojunction photocatalyst prepared by a biomediated route for enhanced hydrogen evolution and Rhodamine B degradation. Materials Chemistry Frontiers, 2017, 1, 1641-1653.	3.2	49
187	Inter-MOF hybrid (IMOFH): A concise analysis on emerging core–shell based hierarchical and multifunctional nanoporous materials. Coordination Chemistry Reviews, 2021, 434, 213786.	9.5	49
188	Surface-Plasmon-Resonance-Induced Photocatalysis by Core–Shell SiO ₂ @Ag NCs@Ag ₃ PO ₄ toward Water-Splitting and Phenol Oxidation Reactions. Inorganic Chemistry, 2019, 58, 9643-9654.	1.9	48
189	Facile synthesis of mesoporous composite Fe/Al2O3–MCM-41: an efficient adsorbent/catalyst for swift removal of methylene blue and mixed dyes. Journal of Materials Chemistry, 2012, 22, 7567.	6.7	47
190	Facile fabrication of mesoporous α-Fe2O3/SnO2 nanoheterostructure for photocatalytic degradation of malachite green. Catalysis Today, 2014, 224, 171-179.	2.2	47
191	Amine functionalized MCM-41: an efficient heterogeneous recyclable catalyst for the synthesis of quinazoline-2,4(1H,3H)-diones from carbon dioxide and 2-aminobenzonitriles in water. Catalysis Science and Technology, 2014, 4, 1608-1614.	2.1	47
192	Dramatic promotion of gold/titania for CO oxidation by sulfate ions. Chemical Communications, 2007, , 1044.	2.2	46
193	Facile fabrication of mesoporosity driven N–TiO2@CS nanocomposites with enhanced visible light photocatalytic activity. RSC Advances, 2013, 3, 4976.	1.7	46
194	Architecting a Double Charge-Transfer Dynamics In ₂ S ₃ /BiVO ₄ n–n Isotype Heterojunction for Superior Photocatalytic Oxytetracycline Hydrochloride Degradation and Water Oxidation Reaction: Unveiling the Association of Physicochemical, Electrochemical, and Photocatalytic Properties. ACS Omega, 2020, 5, 5270-5284.	1.6	46
195	Rationally designed Ti3C2/N, S-TiO2/g-C3N4 ternary heterostructure with spatial charge separation for enhanced photocatalytic hydrogen evolution. Journal of Colloid and Interface Science, 2022, 621, 254-266.	5.0	46
196	Catalytic combustion of volatile organic compounds on Indian Ocean manganese nodules. Applied Catalysis A: General, 1999, 182, 249-256.	2.2	45
197	Effect of phosphate ion on the textural and catalytic activity of titania–silica mixed oxide. Applied Catalysis A: General, 2001, 220, 9-20.	2.2	45
198	Studies on Mg/Fe hydrotalciteâ€ŀike – compound (HTlc): removal of Chromium (VI) from aqueous solution. International Journal of Environmental Studies, 2004, 61, 605-616.	0.7	45

#	Article	IF	CITATIONS
199	Solar Light Active Photodegradation of Phenol over a Fe _{<i>x</i>} Ti _{1â^'<i>x</i>} O _{2â^'<i>y</i>} N _{<i>y</i>} Nanophotocatalyst. Industrial & Engineering Chemistry Research, 2010, 49, 8339-8346.	1.8	45
200	Novel Sm2Ti2O7/SmCrO3 heterojunction based composite photocatalyst for degradation of Rhodamine 6G dye. Chemical Engineering Journal, 2013, 215-216, 608-615.	6.6	45
201	A stable amine functionalized montmorillonite supported Cu, Ni catalyst showing synergistic and co-operative effectiveness towards C–S coupling reactions. RSC Advances, 2013, 3, 7570.	1.7	45
202	Organic amine-functionalized silica-based mesoporous materials: an update of syntheses and catalytic applications. RSC Advances, 2014, 4, 57111-57124.	1.7	45
203	Green exfoliation of graphitic carbon nitride towards decolourization of Congo-Red under solar irradiation. Journal of Environmental Chemical Engineering, 2019, 7, 103456.	3.3	45
204	Photocatalytic activity of sulfate modified titania 3: Decolorization of methylene blue in aqueous solution. Journal of Molecular Catalysis A, 2006, 258, 118-123.	4.8	44
205	{040/110} Facet Isotype Heterojunctions with Monoclinic Scheelite BiVO ₄ . Inorganic Chemistry, 2020, 59, 10328-10342.	1.9	44
206	Visible light active LaFeO3 nano perovskite-RGO-NiO composite for efficient H2 evolution by photocatalytic water splitting and textile dye degradation. Journal of Environmental Chemical Engineering, 2021, 9, 104675.	3.3	44
207	Bandgap engineering <i>via</i> boron and sulphur doped carbon modified anatase TiO ₂ : a visible light stimulated photocatalyst for photo-fixation of N ₂ and TCH degradation. Nanoscale Advances, 2020, 2, 2004-2017.	2.2	43
208	One step towards the 1T/2H-MoS ₂ mixed phase: a journey from synthesis to application. Materials Chemistry Frontiers, 2021, 5, 2143-2172.	3.2	43
209	Review on MXene/TiO2 nanohybrids for photocatalytic hydrogen production and pollutant degradations. Journal of Environmental Chemical Engineering, 2022, 10, 107211.	3.3	43
210	Transition-metal oxide pillared clays. Journal of Materials Chemistry, 1997, 7, 147-152.	6.7	42
211	Low temperature CO oxidation over gold supported mesoporous Fe–TiO2. Journal of Molecular Catalysis A, 2010, 319, 92-97.	4.8	42
212	Enhanced photocatalytic and adsorptive degradation of organic dyes by mesoporous Cu/Al2O3–MCM-41: intra-particle mesoporosity, electron transfer and OH radical generation under visible light. Dalton Transactions, 2011, 40, 7348.	1.6	42
213	Erratic charge transfer dynamics of Au/ZnTiO ₃ nanocomposites under UV and visible light irradiation and their related photocatalytic activities. Nanoscale, 2018, 10, 18540-18554.	2.8	42
214	Effect of anions on the textural and catalytic activity of titania. Journal of Materials Science, 2003, 38, 1835-1848.	1.7	41
215	Isopropylation of benzene over sulfated ZrO2–TiO2 mixed-oxide catalyst. Applied Catalysis A: General, 2003, 243, 271-284.	2.2	41
216	Photo-oxidation of 4-nitrophenol in aqueous suspensions, catalysed by titania intercalated zirconium phosphate (TiP). Journal of Photochemistry and Photobiology A: Chemistry, 2004, 163, 561-567.	2.0	41

#	Article	IF	CITATIONS
217	Studies on MCM-41: Effect of sulfate on nitration of phenol. Journal of Molecular Catalysis A, 2006, 258, 381-387.	4.8	41
218	Schiff Base Pt(II) Complex Intercalated Montmorillonite: A Robust Catalyst for Hydrogenation of Aromatic Nitro Compounds at Room Temperature. Industrial & Engineering Chemistry Research, 2011, 50, 7849-7856.	1.8	41
219	Bio-surfactant assisted solvothermal synthesis of Magnetic retrievable Fe3O4@rGO nanocomposite for photocatalytic reduction of 2-nitrophenol and degradation of TCH under visible light illumination. Applied Surface Science, 2019, 466, 679-690.	3.1	41
220	Studies on Indian Ocean Manganese Nodules. Journal of Colloid and Interface Science, 1996, 181, 456-462.	5.0	40
221	Cesium salts of heteropoly acid immobilized mesoporous silica: An efficient catalyst for acylation of anisole. Journal of Colloid and Interface Science, 2010, 350, 132-139.	5.0	40
222	Cs salt of Co substituted lacunary phosphotungstate supported K10 montmorillonite showing binary catalytic activity. Chemical Engineering Journal, 2013, 215-216, 849-858.	6.6	40
223	Cerium-Based Metal–Organic Framework Nanorods Nucleated on CeO ₂ Nanosheets for Photocatalytic N ₂ Fixation and Water Oxidation. ACS Applied Nano Materials, 2021, 4, 9635-9652.	2.4	40
224	Transition metal pillared clay 4. A comparative study of textural, acidic and catalytic properties of chromia pillared montmorillonite and acid activated montmorillonite. Applied Catalysis A: General, 1998, 166, 123-133.	2.2	39
225	Studies on anion-promoted titania. Journal of Molecular Catalysis A, 2001, 176, 151-163.	4.8	39
226	Studies on manganese-nodule leached residues. Journal of Colloid and Interface Science, 2004, 277, 48-54.	5.0	39
227	Surface characterization and catalytic evaluation of copper-promoted Al-MCM-41 toward hydroxylation of phenol. Journal of Colloid and Interface Science, 2009, 340, 209-217.	5.0	39
228	Removal of phenolic compounds from aqueous solutions by adsorption onto manganese nodule leached residue. Journal of Hazardous Materials, 2010, 173, 758-764.	6.5	39
229	Gd ₂ Ti ₂ O ₇ /In ₂ O ₃ : Efficient Visibleâ€Lightâ€Driven Heterojunctionâ€Based Composite Photocatalysts for Hydrogen Production. ChemCatChem, 2013, 5, 2352-2359.	1.8	39
230	Heterojunction conception of n-La2Ti2O7/p-CuO in the limelight of photocatalytic formation of hydrogen under visible light. RSC Advances, 2014, 4, 14633.	1.7	39
231	Stupendous Photocatalytic Activity of p-BiOI/n-PbTiO3 Heterojunction: The Significant Role of Oxygen Vacancies and Interface Coupling. Journal of Physical Chemistry C, 2019, 123, 21593-21606.	1.5	39
232	Fabrication, Characterization, and Photoelectrochemical Properties of Cuâ€Doped PbTiO ₃ and Its Hydrogen Production Activity. ChemCatChem, 2013, 5, 3812-3820.	1.8	38
233	Reduced Graphene Oxide/InGaZn Mixed Oxide Nanocomposite Photocatalysts for Hydrogen Production. ChemSusChem, 2014, 7, 585-597.	3.6	38
234	Quantum confinement chemistry of CdS QDs plus hot electron of Au over TiO2 nanowire protruding to be encouraging photocatalyst towards nitrophenol conversion and ciprofloxacin degradation. Journal of Environmental Chemical Engineering, 2019, 7, 102821.	3.3	38

#	Article	IF	CITATIONS
235	A Mechanistic Approach on Oxygen Vacancy-Engineered CeO ₂ Nanosheets Concocts over an Oyster Shell Manifesting Robust Photocatalytic Activity toward Water Oxidation. ACS Omega, 2020, 5, 9789-9805.	1.6	38
236	Studies on MnO2—II. Relationship between physicochemical properties and electrochemical activity of some synthetic MnO2 of different crystallographic forms. Electrochimica Acta, 1981, 26, 1147-1156.	2.6	37
237	Interfacial behavior of some synthetic MnO2 samples during their adsorption of Cu2+ and Ba2+ from aqueous solution at 300°K. Journal of Colloid and Interface Science, 1984, 98, 252-260.	5.0	37
238	A facile method for the synthesis of copper modified amine-functionalized mesoporous zirconia and its catalytic evaluation in C–S coupling reaction. Dalton Transactions, 2011, 40, 9169.	1.6	37
239	A simple and efficient protocol using palladium based lacunary phosphotungstate supported mesoporous silica towards hydrogenation of p-nitrophenol to p-aminophenol at room temperature. Catalysis Science and Technology, 2012, 2, 979.	2.1	37
240	Influence of Au/Pd alloy on an amine functionalised ZnCr LDH–MCM-41 nanocomposite: A visible light sensitive photocatalyst towards one-pot imine synthesis. Catalysis Science and Technology, 2019, 9, 2493-2513.	2.1	37
241	Studies on Ferric Oxide Hydroxides. Journal of Colloid and Interface Science, 1996, 178, 586-593.	5.0	36
242	Transition Metal Oxide Pillared Clay. Journal of Colloid and Interface Science, 1996, 183, 176-183.	5.0	36
243	Transition metal pillared clay:. Journal of Molecular Catalysis A, 1997, 121, 91-96.	4.8	36
244	Studies on heteropoly acid supported zirconia. Journal of Molecular Catalysis A, 2007, 261, 172-179.	4.8	36
245	Hydroxylation of phenol over molybdovanadophosphoric acid modified zirconia. Journal of Molecular Catalysis A, 2008, 279, 104-111.	4.8	36
246	Visible light response photocatalytic water splitting over CdS-pillared zirconium–titanium phosphate (ZTP). International Journal of Hydrogen Energy, 2010, 35, 5262-5269.	3.8	36
247	A facile method for promoting activities of vanadium–schiffbase complex anchored on organically modified MCM-41 in epoxidation reaction. Journal of Molecular Catalysis A, 2010, 325, 40-47.	4.8	36
248	Facile synthesis of InGaZn mixed oxide nanorods for enhanced hydrogen production under visible light. Dalton Transactions, 2012, 41, 14107.	1.6	36
249	Glimpses of the modification of perovskite with graphene-analogous materials in photocatalytic applications. Inorganic Chemistry Frontiers, 2015, 2, 807-823.	3.0	36
250	Rational Design of a Coupled Confronting Z‣cheme System Toward Photocatalytic Refractory Pollutant Degradation and Water Splitting Reaction. Advanced Materials Interfaces, 2019, 6, 1900370.	1.9	36
251	Discriminatory {040}-Reduction Facet/Ag ⁰ Schottky Barrier Coupled {040/110}-BiVO ₄ @Ag@CoAl-LDH Z-Scheme Isotype Heterostructure. Inorganic Chemistry, 2021, 60, 1698-1715.	1.9	36
252	ZnFe ₂ O ₄ @WO _{3–<i>X</i>} /Polypyrrole: An Efficient Ternary Photocatalytic System for Energy and Environmental Application. ACS Omega, 2021, 6, 30401-30418.	1.6	36

#	Article	IF	CITATIONS
253	Incorporating nitrogen vacancies in exfoliated B-doped g-C ₃ N ₄ towards improved photocatalytic ciprofloxacin degradation and hydrogen evolution. New Journal of Chemistry, 2022, 46, 3493-3503.	1.4	36
254	Aggrandizing the Photoactivity of ZnO Nanorods toward N ₂ Reduction and H ₂ Evolution through Facile <i>In Situ</i> Coupling with Ni <i>_x</i> P <i>_y</i> . ACS Sustainable Chemistry and Engineering, 2021, 9, 6305-6317.	3.2	35
255	An insight to band-bending mechanism of polypyrrole sensitized B-rGO/ZnFe2O4 p-n heterostructure with dynamic charge transfer for photocatalytic applications. International Journal of Hydrogen Energy, 2021, 46, 24484-24500.	3.8	35
256	Esterification of acetic acid with n-butanol over manganese nodule leached residue. Journal of Molecular Catalysis A, 2007, 266, 88-92.	4.8	34
257	Adsorption of Cu2+ on spherical Fe-MCM-41 and its application for oxidation of adamantane. Journal of Hazardous Materials, 2010, 179, 642-649.	6.5	34
258	Visible light induced photo-hydroxylation of phenol to catechol over RGO–Ag3VO4 nanocomposites without the use of H2O2. RSC Advances, 2012, 2, 7377.	1.7	34
259	Solar light driven Rhodamine B degradation over highly active β-SiC–TiO ₂ nanocomposite. RSC Advances, 2014, 4, 12918-12928.	1.7	34
260	Palladium anchored on amine-functionalized K10 as an efficient, heterogeneous and reusable catalyst for carbonylative Sonogashira reaction. Applied Catalysis A: General, 2015, 506, 237-245.	2.2	34
261	Recent Advances on Alloyed Quantum Dots for Photocatalytic Hydrogen Evolution: A Mini-Review. Energy & Fuels, 2021, 35, 4670-4686.	2.5	34
262	Transition metal oxide pillared clay: 5. Synthesis, characterisation and catalytic activity of iron–chromium mixed oxide pillared montmorillonite. Applied Catalysis A: General, 1998, 174, 91-98.	2.2	33
263	SO42â^'/TiO2-SiO2 mixed oxide catalyst. Applied Catalysis A: General, 2001, 211, 175-187.	2.2	33
264	Effect of heat treatment on the physico-chemical properties and catalytic activity of manganese nodules leached residue towards decomposition of hydrogen peroxide. Journal of Colloid and Interface Science, 2005, 290, 431-436.	5.0	33
265	Amine modified mesoporous Al ₂ O ₃ @MCM-41: an efficient, synergetic and recyclable catalyst for the formylation of amines using carbon dioxide and DMAB under mild reaction conditions. Catalysis Science and Technology, 2016, 6, 4872-4881.	2.1	33
266	Enhanced Photocatalytic Activity of a Molybdateâ€Intercalated Ironâ€Based Layered Double Hydroxide. European Journal of Inorganic Chemistry, 2017, 2017, 723-733.	1.0	33
267	Studies on Anion Promoted Titania.1: Preparation, Characterization, and Catalytic Activity toward Alcohol and Cumene Conversion Reactions of Phosphated Titania. Journal of Colloid and Interface Science, 1999, 217, 388-394.	5.0	32
268	Synthesis, characterization and catalytic activity of copper incorporated and immobilized mesoporous MCM-41 in the single step amination of benzene. Journal of Molecular Catalysis A, 2010, 318, 85-93.	4.8	32
269	Studies on PO3â ^{°°} 4/ZrO2. Journal of Colloid and Interface Science, 1996, 182, 381-387.	5.0	31
270	Modified TiO2–SiO2 mixed oxides. Applied Catalysis B: Environmental, 2005, 57, 83-91.	10.8	31

#	Article	IF	CITATIONS
271	ZnFe ₂ O ₄ â€Decorated Mesoporous Al ₂ O ₃ Modified MCMâ€41: A Solarâ€Lightâ€Active Photocatalyst for the Effective Removal of Phenol and Cr (VI) from Water. ChemistrySelect, 2019, 4, 1806-1819.	0.7	31
272	Boosting sluggish photocatalytic hydrogen evolution through piezo-stimulated polarization: a critical review. Materials Horizons, 2022, 9, 1332-1355.	6.4	31
273	Studies on Indian Ocean Manganese Nodules. Journal of Colloid and Interface Science, 1995, 173, 112-118.	5.0	30
274	Photocatalytic decolorisation of methylene blue (MB) over titania pillared zirconium phosphate (ZrP) and titanium phosphate (TiP) under solar radiation. Journal of Molecular Catalysis A, 2007, 261, 254-261.	4.8	30
275	Influence of secondary oxide phases in enhancing the photocatalytic properties of alkaline earth elements doped LaFeO3 nanocomposites. Journal of Physics and Chemistry of Solids, 2020, 140, 109377.	1.9	30
276	HERs in an acidic medium over MoS ₂ nanosheets: from fundamentals to synthesis and the recent progress. Sustainable Energy and Fuels, 2021, 5, 1952-1987.	2.5	30
277	Catalytic Ketonization of Acetic Acid on Zn/Al Layered Double Hydroxides. Reaction Kinetics and Catalysis Letters, 2000, 69, 223-229.	0.6	29
278	One-pot synthesis of 5-hydroxymethylfurfural: a significant biomass conversion over tin-promoted vanadium phosphate (Sn–VPO) catalyst. Catalysis Science and Technology, 2013, 3, 3278.	2.1	29
279	Acylation of anisole over 12-heteropolyacid of tungsten and molybdenum promoted zirconia. Journal of Molecular Catalysis A, 2009, 297, 93-100.	4.8	28
280	Mesoporous nanocomposite Fe/Al2O3–MCM-41: An efficient photocatalyst for hydrogen production under visible light. International Journal of Hydrogen Energy, 2011, 36, 12753-12760.	3.8	28
281	Facile Synthesis of Bi ₂ O ₃ /TiO _{2â^³<i>x</i>} N _{<i>x</i>} and its Direct Solarâ€Lightâ€Driven Photocatalytic Selective Hydroxylation of Phenol. ChemCatChem, 2011, 3, 311-318.	1.8	28
282	Enhanced photodegradation of dyes and mixed dyes by heterogeneous mesoporous Co–Fe/Al ₂ O ₃ –MCM-41 nanocomposites: nanoparticles formation, semiconductor behavior and mesoporosity. RSC Advances, 2016, 6, 94263-94277.	1.7	28
283	Dynamic charge transfer through Fermi level equilibration in the p-CuFe ₂ O ₄ /n-NiAl LDH interface towards photocatalytic application. Catalysis Science and Technology, 2020, 10, 6285-6298.	2.1	28
284	Effect of microemulsion composition on textural and photocatalytic activity of titania nanomaterial. Applied Catalysis A: General, 2006, 310, 183-189.	2.2	27
285	Selective nitration of phenol over silicotungstic acid supported zirconia. Catalysis Communications, 2007, 8, 1487-1492.	1.6	27
286	Incorporation of Silver Ions into Zirconium Titanium Phosphate: A Novel Approach toward Antibacterial Activity. Industrial & Engineering Chemistry Research, 2011, 50, 9479-9486.	1.8	27
287	Facile fabrication of aluminum-promoted vanadium phosphate: A highly active heterogeneous catalyst for isopropylation of toluene to cymene. Journal of Catalysis, 2012, 289, 190-198.	3.1	27
288	Facile Fabrication Of RGO/N-GZ Mixed Oxide Nanocomposite For Efficient Hydrogen Production Under Visible Light. Journal of Physical Chemistry C, 2015, 119, 6634-6646.	1.5	27

#	Article	IF	CITATIONS
289	Functional facet isotype junction and semiconductor/r-GO minor Schottky barrier tailored In2S3@r-GO@(040/110)-BiVO4 ternary hybrid. Journal of Colloid and Interface Science, 2021, 585, 519-537.	5.0	27
290	Adsorptive removal of Cr(VI) onto UiO-66-NH2 and its determination by radioanalytical techniques. Journal of Radioanalytical and Nuclear Chemistry, 2019, 322, 983-992.	0.7	27
291	Studies on sulphated zirconia: synthesis, physico-chemical characterisation and n-butane isomerisation activity. Applied Catalysis A: General, 2002, 224, 179-189.	2.2	26
292	Mechanistic aspects of enhanced congo red adsorption over graphene oxide in presence of methylene blue. Journal of Environmental Chemical Engineering, 2016, 4, 3498-3511.	3.3	26
293	Black titania an emerging photocatalyst: review highlighting the synthesis techniques and photocatalytic activity for hydrogen generation. Nanoscale Advances, 2021, 3, 5487-5524.	2.2	26
294	Cation Exchange and Sorption Properties of Aluminum Phosphate. Separation Science and Technology, 1998, 33, 1057-1073.	1.3	25
295	Liquid phase bromination of phenol. Applied Catalysis A: General, 2006, 305, 32-38.	2.2	25
296	Effect of sulfate on the surface and catalytic properties of iron–chromium mixed oxide pillared clay. Journal of Colloid and Interface Science, 2006, 301, 554-559.	5.0	25
297	Studies on heteropoly acid supported zirconia II. Liquid phase bromination of phenol and various organic substrates. Catalysis Communications, 2007, 8, 889-893.	1.6	25
298	Facile Method for Synthesis of Polyamine-Functionalized Mesoporous Zirconia and Its Catalytic Evaluation toward Henry Reaction. Industrial & Engineering Chemistry Research, 2011, 50, 2055-2064.	1.8	25
299	Sulphated zirconia: an efficient paraselectivecatalyst for mononitration of halobenzenes. Catalysis Letters, 1997, 47, 255-257.	1.4	24
300	Catalytic ketonization of monocarâ~ylic acids over Indian Ocean manganese nodules. Applied Catalysis A: General, 1998, 166, 201-205.	2.2	24
301	SO2â^'4/TiO2–SiO2 Mixed Oxide Catalyst, I: Synthesis, Characterization, and Acidic Properties. Journal of Colloid and Interface Science, 1999, 216, 127-133.	5.0	24
302	Selective gas phase oxidation of methanol to formaldehyde over aluminum promoted vanadium phosphate. Chemical Engineering Journal, 2012, 180, 270-276.	6.6	24
303	Solventâ€Switchable Regioselective Synthesis of Aurones and Flavones Using Palladiumâ€Supported Amineâ€Functionalized Montmorillonite as a Heterogeneous Catalyst. ChemCatChem, 2016, 8, 2649-2658.	1.8	24
304	MoS2-mesoporous LaFeO3 hybrid photocatalyst: Highly efficient visible-light driven photocatalyst. International Journal of Hydrogen Energy, 2020, 45, 11502-11511.	3.8	24
305	A study on the structural properties of mesoporous silica spheres. Materials Letters, 2007, 61, 3942-3945.	1.3	23
306	CuxH3â^'2xPW12O40Supported on MCM-41: Their Activity to Heck Vinylation of Aryl Halides. Industrial & Engineering Chemistry Research, 2010, 49, 8942-8948.	1.8	23

#	Article	IF	CITATIONS
307	Amine functionalized layered double hydroxide: a reusable catalyst for aldol condensation. New Journal of Chemistry, 2011, 35, 2503.	1.4	23
308	Liquid phase esterification of acetic acid over WO3 promoted Î ² -SiC in a solvent free system. Dalton Transactions, 2012, 41, 14299.	1.6	23
309	Facile fabrication of mesoporous iron modified Al2O3 nanoparticles pillared montmorillonite nanocomposite: a smart photo-Fenton catalyst for quick removal of organic dyes. Dalton Transactions, 2013, 42, 15139.	1.6	23
310	Enhanced hydrogen production over CdSe QD/ZTP composite under visible light irradiation without using co-catalyst. International Journal of Hydrogen Energy, 2013, 38, 1267-1277.	3.8	23
311	Pd(II) loaded on diamine functionalized LDH for oxidation of primary alcohol using water as solvent. Applied Catalysis A: General, 2013, 460-461, 36-45.	2.2	23
312	Fabrication of the Mesoporous Fe@MnO ₂ NPs–MCM-41 Nanocomposite: An Efficient Photocatalyst for Rapid Degradation of Phenolic Compounds. Journal of Physical Chemistry C, 2015, 119, 14145-14159.	1.5	23
313	A review on g-C ₃ N ₄ /graphene nanocomposites: multifunctional roles of graphene in the nanohybrid photocatalyst toward photocatalytic applications. Catalysis Science and Technology, 2021, 11, 6018-6040.	2.1	23
314	MgCr-LDH Nanoplatelets as Effective Oxidation Catalysts for Visible Light-Triggered Rhodamine B Degradation. Catalysts, 2021, 11, 1072.	1.6	23
315	Superlative photoelectrochemical properties of 3D MgCr-LDH nanoparticles influencing towards photoinduced water splitting reactions. Scientific Reports, 2022, 12, .	1.6	23
316	Studies on PO43â°'/ZrO2. Journal of Colloid and Interface Science, 2000, 226, 340-345.	5.0	22
317	Freeze-dried promoted and unpromoted sulfated zirconia and their catalytic potential. Journal of Materials Chemistry, 2001, 11, 1903-1911.	6.7	22
318	Facile Method for the Synthesis of Phosphomolybdic Acid Supported on Zirconia–Ceria Mixed Oxide and Its Catalytic Evaluation in the Solvent-Free Oxidation of Benzyl Alcohol. Industrial & Engineering Chemistry Research, 2012, 51, 7859-7866.	1.8	22
319	Fabrication of NiO/Ta2O5composite photocatalyst for hydrogen production under visible light. International Journal of Energy Research, 2013, 37, 161-170.	2.2	22
320	Recent advances in wireless photofixation of dinitrogen to ammonia under the ambient condition: A review. Journal of Photochemistry and Photobiology C: Photochemistry Reviews, 2021, 47, 100402.	5.6	22
321	Construction of NiCo ₂ O ₄ /O-g-C ₃ N ₄ Nanocomposites: A Battery-Type Electrode Material for High-Performance Supercapacitor Application. ACS Applied Nano Materials, 2021, 4, 10173-10184.	2.4	22
322	Metal organic framework-based Janus nanomaterials: rational design, strategic fabrication and emerging applications. Dalton Transactions, 2022, 51, 5352-5366.	1.6	22
323	Studies on Indian Ocean Manganese Nodules. Journal of Colloid and Interface Science, 1997, 187, 375-380.	5.0	21
324	Cation Exchange and Sorption Properties of TIN(IV) Phosphate. Journal of Colloid and Interface Science, 2000, 225, 511-519.	5.0	21

#	Article	IF	CITATIONS
325	A reusable Mn(ii)-dampy-MCM-41 system for single step amination of benzene to aniline using hydroxylamine. Catalysis Science and Technology, 2011, 1, 1496.	2.1	21
326	A facile method for synthesis of Keggin-type cesium salt of iron substituted lacunary phosphotungstate supported on MCM-41 and study of its extraordinary catalytic activity. Catalysis Today, 2012, 198, 52-58.	2.2	21
327	Photocatalytic activity of Au/TiO2 nanocomposite for azo-dyes degradation. Kinetics and Catalysis, 2012, 53, 197-205.	0.3	21
328	Engineering an oxygen-vacancy-mediated step-scheme charge carrier dynamic coupling WO _{3â^'<i>X</i>} /ZnFe ₂ O ₄ heterojunction for robust photo-Fenton-driven levofloxacin detoxification. New Journal of Chemistry, 2022, 46, 5785-5798.	1.4	21
329	Transition metal promoted AlPO4 catalyst 2. The catalytic activity of M0.05Al0.95PO4 for alcohol conversion and cumene cracking/dehydrogenation reactions. Applied Catalysis A: General, 1998, 166, 115-122.	2.2	20
330	Studies on Indian Ocean Manganese Nodules. VIII. Adsorption of Aqueous Phosphate on Ferromanganese Nodules. Journal of Colloid and Interface Science, 1998, 199, 22-27.	5.0	20
331	Studies on manganese nodule leached residues. Journal of Colloid and Interface Science, 2005, 290, 22-27.	5.0	20
332	Studies on selenite adsorption using manganese nodule leached residues. Journal of Colloid and Interface Science, 2007, 307, 333-339.	5.0	20
333	Enhanced electrochemical performance of flexible asymmetric supercapacitor based on novel nanostructured activated fullerene anchored zinc cobaltite. Journal of Alloys and Compounds, 2022, 919, 165753.	2.8	20
334	Visible light active titanate perovskites: An overview on its synthesis, characterization and photocatalytic applications. Materials Research Bulletin, 2022, 155, 111965.	2.7	20
335	Sol–gel synthesis and characterization of mesoporous iron–titanium mixed oxide for catalytic application. Materials Chemistry and Physics, 2010, 123, 427-433.	2.0	19
336	Fascinating and challenging role of tungstate promoted vanadium phosphate towards solvent free esterification of oleic acid. Dalton Transactions, 2012, 41, 1325-1331.	1.6	19
337	A review on dimensionally controlled synthesis of g-C ₃ N ₄ and formation of an isotype heterojunction for photocatalytic hydrogen evolution. Catalysis Science and Technology, 2021, 11, 7505-7524.	2.1	19
338	Robust direct Z-scheme exciton transfer dynamics by architecting 3D BiOI MF-supported non-stoichiometric Cu _{0.75} In _{0.25} S NC nanocomposite for co-catalyst-free photocatalytic hydrogen evolution. RSC Advances, 2022, 12, 1265-1277.	1.7	19
339	Amine-modified titania–silica mixed oxides: 1. Effect of amine concentration and activation temperature towards epoxidation of cyclohexene. Catalysis Communications, 2005, 6, 578-581.	1.6	18
340	Mn(III) oxide pillared titanium phosphate (TiP) for catalytic deep oxidation of VOCs. Applied Catalysis A: General, 2007, 324, 1-8.	2.2	18
341	A fascinating Suzuki homo-coupling reaction over anchored gold Schiff base complexes on mesoporous host. Journal of Molecular Catalysis A, 2011, 342-343, 11-17.	4.8	18
342	Enhanced photocatalytic activity over N-doped GaZn mixed oxide under visible light irradiation. International Journal of Hydrogen Energy, 2012, 37, 115-124.	3.8	18

#	Article	IF	CITATIONS
343	Fabrication of Amine and Zirconia on MCMâ€41 as Acid–Base Catalysts for the Fixation of Carbon Dioxide. ChemCatChem, 2017, 9, 4105-4111.	1.8	18
344	Crystal facet and surface defect engineered low dimensional CeO ₂ (0D, 1D, 2D) based photocatalytic materials towards energy generation and pollution abatement. Materials Advances, 2021, 2, 6942-6983.	2.6	18
345	Studies on ?-FeOOH. Journal of Materials Science, 1988, 23, 1201-1205.	1.7	17
346	Liquid phase bromination of phenol over titania pillared zirconium phosphate and titanium phosphate. Catalysis Communications, 2006, 7, 68-72.	1.6	17
347	Liquid phase bromination of phenol. Journal of Molecular Catalysis A, 2006, 253, 70-78.	4.8	17
348	A comparative study of molybdenum promoted vanadium phosphate catalysts towards epoxidation of cyclohexene. Applied Catalysis A: General, 2013, 464-465, 364-373.	2.2	17
349	Organocatalytic Cascade Knoevenagel–Michael Addition Reactions: Direct Synthesis of Polysubstituted 2-Amino-4H-Chromene Derivatives. Catalysis Letters, 2020, 150, 2331-2351.	1.4	17
350	Robust charge carrier engineering <i>via</i> plasmonic effect and conjugated Î-framework on Au loaded ZnCr-LDH/RGO photocatalyst towards H ₂ and H ₂ O ₂ production. Inorganic Chemistry Frontiers, 2022, 9, 559-576.	3.0	17
351	The effect of the thermal stability of some synthetic MnO2 samples on their electrochemical and catalytic activity. Thermochimica Acta, 1983, 64, 131-138.	1.2	16
352	High surface area silicon carbide from rice husk: A support material for catalysts. Reaction Kinetics and Catalysis Letters, 1995, 54, 29-34.	0.6	16
353	Studies on ferric oxide hydroxides. Journal of Materials Science, 1996, 31, 2199-2205.	1.7	16
354	Low temperature CO adsorption and oxidation over Au/rare earth-TiO2 nanocatalysts. Applied Catalysis A: General, 2011, 399, 110-116.	2.2	16
355	Fabrication of nano N-doped In2Ga2ZnO7 for photocatalytic hydrogen production under visible light. International Journal of Hydrogen Energy, 2012, 37, 17936-17946.	3.8	16
356	Calculation of relative fluorescence quantum yield and Urbach energy of colloidal CdS QDs in various easily accessible solvents. Journal of Luminescence, 2021, 231, 117792.	1.5	16
357	Facile fabrication of nano silver phosphate on B-doped g-C3N4: An excellent p-n heterojunction photocatalyst towards water oxidation and Cr (VI) reduction. Journal of Alloys and Compounds, 2022, 898, 162853.	2.8	16
358	Mechanistic insight the visible light driven hydrogen generation by plasmonic Au-Cu alloy mounted on TiO2 @B-doped g-C3N4 heterojunction photocatalyst. Journal of Alloys and Compounds, 2022, 909, 164754.	2.8	16
359	Effect of perchlorate ion on the textural and catalytic activity of zirconia. Applied Catalysis A: General, 1999, 184, 219-229.	2.2	15
360	Iron, and Manganese Doped SO42-/ZrO2–TiO2Mixed Oxide Catalysts: Studies on Acidity and Benzene Isopropylation Activity. Catalysis Letters, 2004, 93, 185-193.	1.4	15

#	Article	IF	CITATIONS
361	Phosphotungstic acid promoted zirconia–alumina mixed oxides: A stable and reusable catalysts for epoxidation of trans-stilbene. Catalysis Communications, 2009, 11, 51-57.	1.6	15
362	A Facile Synthesis of Vanadium Phosphate: An Efficient Catalyst for Solvent Free Esterification of Acetic Acid. Catalysis Letters, 2010, 140, 197-204.	1.4	15
363	Facile Synthesis of Dodecatungstophosphoric Acid @ TiO2 Pillared Montmorillonite and Its Effectual Exploitation Towards Solvent Free Esterification of Acetic Acid with n-Butanol. Catalysis Letters, 2011, 141, 1476-1483.	1.4	15
364	Selective oxidation of benzaldehyde by molecular oxygen over molybdovanadophosphoric acid supported MCM-41. Journal of Porous Materials, 2012, 19, 397-404.	1.3	15
365	Visible-light-induced water reduction reaction for efficient hydrogen production by N-doped In ₂ Ga ₂ ZnO ₇ nanoparticle decorated on RGO sheets. Inorganic Chemistry Frontiers, 2016, 3, 1582-1596.	3.0	15
366	A Visible Light-Driven Zn/Cr-LaFeO ₃ Nanocomposite with Enhanced Photocatalytic Activity towards H ₂ Production and RhB Degradation. ChemistrySelect, 2017, 2, 10239-10248.	0.7	15
367	Smart 2D-2D Nano-Composite Adsorbents of LDH-Carbonaceous Materials for the Removal of Aqueous Toxic Heavy Metal Ions: A Review. Current Environmental Engineering, 2018, 5, 20-34.	0.6	15
368	Adsorption of Cu2+ on various crystalline modifications of MnO2 at 300°K. Journal of Colloid and Interface Science, 1984, 98, 245-251.	5.0	14
369	Transition Metal Promoted Amorphous AlPO4Catalysts 1. Acid–Base and Textural Properties. Journal of Colloid and Interface Science, 1996, 179, 233-240.	5.0	14
370	Title is missing!. Reaction Kinetics and Catalysis Letters, 2003, 78, 381-387.	0.6	14
371	Chemoselective oxidation of primary alcohols catalysed by Ce(iii)-complex intercalated LDH using molecular oxygen at room temperature. Dalton Transactions, 2011, 40, 11838.	1.6	14
372	Characterization of novel Cs and K substituted phosphotungstic acid modified MCM-41 catalyst and its catalytic activity towards acetylation of aromatic alcohols. Journal of Chemical Sciences, 2012, 124, 1117-1125.	0.7	14
373	Phosphorous, boron and sulfur doped g-C3N4 nanosheet: Synthesis, characterization, and comparative study towards photocatalytic hydrogen generation. Materials Today: Proceedings, 2021, 35, 258-262.	0.9	14
374	Studies on structural properties, surface acidity and benzene isopropylation activity of sulphated ZrO2–TiO2 mixed oxide catalysts. Microporous and Mesoporous Materials, 2005, 80, 327-336.	2.2	13
375	Using phosphorus doping of MoO3/ZSM-5 to modify performance in methane dehydroaromatisation. Journal of Molecular Catalysis A, 2006, 245, 141-146.	4.8	13
376	Anchoring of Fe(III)salicylamide onto MCM-41 for Catalytic Hydroxylation of Phenol in Aqueous Medium Using Hydrogen Peroxide as Oxidant. Catalysis Letters, 2010, 136, 155-163.	1.4	13
377	La Complex@Fe–PILM Offering Resilient Option for Efficient and Green Processing toward Epoxidation of Cyclohexene. Industrial & Engineering Chemistry Research, 2011, 50, 8973-8982.	1.8	13
378	Tungstate promoted vanadium phosphate catalysts for the gas phase oxidation of methanol to formaldehyde. Catalysis Science and Technology, 2013, 3, 1558.	2.1	13

#	Article	IF	CITATIONS
379	Sustainable nano composite of mesoporous silica supported red mud for solar powered degradation of aquatic pollutants. Journal of Environmental Chemical Engineering, 2017, 5, 6137-6147.	3.3	13
380	Thermal transformation of trinuclear Fe(III) acetato complex intercalated montmorillonite. Applied Clay Science, 1999, 15, 463-475.	2.6	12
381	Preparation, characterisation of molybdophosphoric and tungstophosphoric acid intercalated zinc aluminium hydrotalcite-like compounds and their catalytic evaluation towards the oxidative bromination of phenol. Catalysis Communications, 2006, 7, 913-919.	1.6	12
382	Solar Light Induced Photocatalytic Degradation of Pollutants over Titania Pillared Zirconium Phosphate and Titanium Phosphate. Catalysis Surveys From Asia, 2008, 12, 203-213.	1.0	12
383	Enhanced Catalytic Activity of Ti, V, Mn-Grafted Silica Spheres Towards Epoxidation Reaction. Catalysis Letters, 2009, 128, 111-118.	1.4	12
384	Superior photocatalytic performance of Co Al LDH in the race of metal incorporated LDH: A comparison study. Materials Today: Proceedings, 2021, 35, 275-280.	0.9	12
385	Thermal decomposition characteristics in air and their relationship with electrochemical activity of different polymorphic forms of MnO2. Thermochimica Acta, 1983, 66, 275-287.	1.2	11
386	Sulfated nanozirconia: an investigation on acid–base properties and n-butane isomerization activity. Journal of Colloid and Interface Science, 2004, 272, 378-383.	5.0	11
387	Fe(III)-salim anchored MCM-41: synthesis, characterization and catalytic activity towards liquid phase cyclohexane oxidation. Journal of Porous Materials, 2011, 18, 707-714.	1.3	11
388	Dramatic enhancement of catalytic activity over transition metal substituted hematite. Journal of Industrial and Engineering Chemistry, 2012, 18, 1612-1619.	2.9	11
389	Sustainable and efficient protocol for the synthesis of a RGO–VPO composite with synergetic stability and reactivity. RSC Advances, 2013, 3, 4863.	1.7	11
390	Photocatalytic and photo-electrochemical ammonia synthesis over dimensional oriented cobalt titanate/nitrogen-doped reduced graphene oxide junction interface catalyst. Journal of Colloid and Interface Science, 2022, 625, 83-99.	5.0	11
391	Studies on Indian Ocean Manganese Nodules PART 2. Physico-chemical Characteristics and Catalytic Activity of Heat-Treated Marine Manganese Nodules. Journal of Colloid and Interface Science, 1996, 179, 241-248.	5.0	10
392	Tungstate-modified aluminium phosphate. Journal of Molecular Catalysis A, 2000, 164, 217-223.	4.8	10
393	Butane isomerization over persulfated zirconia. Applied Catalysis A: General, 2001, 217, 263-273.	2.2	10
394	Liquid Phase Hydrodechlorination of Chlorobenzene over Bimetallic Supported Zirconia Catalyst. Industrial & Engineering Chemistry Research, 2011, 50, 12439-12448.	1.8	10
395	Pillared Clay as an Effective Catalyst for Low Temperature VOCs Decomposition. Key Engineering Materials, 2013, 571, 71-91.	0.4	10
396	Cesium salts of manganese based lacunary phosphotungstate supported mesoporous silica: An efficient catalyst for solvent free oxidation reaction. Catalysis Communications, 2015, 59, 73-77.	1.6	10

#	Article	IF	CITATIONS
397	Enhanced photocatalytic activity of nanoporous BiVO 4 /MCM-41 co-joined nanocomposites for solar energy conversion and environmental pollution abatement. Journal of Environmental Chemical Engineering, 2017, 5, 4524-4530.	3.3	10
398	Unexpected rapid photo-catalytic decolourisation/degradation of organic pollutants over highly active hetero junction based vanadium phosphate catalyst. Catalysis Today, 2017, 284, 84-91.	2.2	10
399	Sulphated Al-MCM-41: A simple, efficient and recyclable catalyst for synthesis of substituted aryl ketones/olefins via alcohols addition to alkynes and coupling with styrenes. Molecular Catalysis, 2018, 452, 46-53.	1.0	10
400	Facile construction of CoWO4 modified g-C3N4 nanocomposites with enhanced photocatalytic activity under visible light irradiation. Materials Today: Proceedings, 2021, 35, 193-197.	0.9	10
401	Systematic investigation on the charge storage behavior of GdCrO3 in aqueous electrolyte. Journal of Energy Storage, 2021, 42, 103145.	3.9	10
402	Energy band modulation in CuxP(x=3,1/2)/PbTiO3 via heterogeneous erection induced benign junction interface for enhanced photocatalytic H2 evolution. International Journal of Hydrogen Energy, 2022, 47, 3893-3905.	3.8	10
403	A concise discussion on MoS ₂ basal plane activation toward the ennoblement of electrocatalytic HER output. Sustainable Energy and Fuels, 2022, 6, 937-953.	2.5	10
404	Robust Photoelectrochemical Route for the Ambient Fixation of Dinitrogen into Ammonia over a Nanojunction Assembled from Ceria and an Iron Boride/Phosphide Cocatalyst. Inorganic Chemistry, 2022, 61, 131-140.	1.9	10
405	CIS QDs nucleated on oxygen vacancy rich BOI microplates: a hybrid photocatalyst with enhanced green energy production <i>via</i> mediator free Z-scheme dynamics. Energy Advances, 2022, 1, 422-437.	1.4	10
406	Application of statistical design of experiments in the study of dissolution of Goethite (α-FeOOH) in hydrochloric acid in the presence of ascorbic acid. Hydrometallurgy, 1997, 46, 271-275.	1.8	9
407	A Glimpse on the plethora of applications of prodigious material MXene. Sustainable Materials and Technologies, 2022, 32, e00439.	1.7	9
408	Removal Of Aqueous Selenite Using Alumina. International Journal of Environmental Studies, 2003, 60, 75-86.	0.7	8
409	Effect of anions on the textural and catalytic activity of titania-silica mixed oxide. Journal of Materials Science, 2004, 39, 3549-3562.	1.7	8
410	Surface characterization and catalytic evaluation of manganese nodule leached residue toward oxidation of benzene to phenol. Journal of Colloid and Interface Science, 2007, 316, 541-546.	5.0	8
411	Fe(III) oxide pillared titanium phosphate (TiP): An effective catalyst for deep oxidation of VOCs. Journal of Molecular Catalysis A, 2007, 276, 17-23.	4.8	8
412	CdS QD Decorated LaFeO 3 Nanosheets for Photocatalytic Application Under Visible Light Irradiation. ChemistrySelect, 2020, 5, 6153-6161.	0.7	8
413	Adsorptive remediation of Cr (VI) from aqueous solution using cobalt ferrite: Kinetics and isotherm studies. Materials Today: Proceedings, 2020, 30, 289-293.	0.9	8
414	Novel synthesis of boron nitride nanosheets from hexagonal boron nitride by modified aqueous phase bi-thermal exfoliation method. Materials Today: Proceedings, 2021, 35, 239-242.	0.9	8

#	Article	IF	CITATIONS
415	Prominence of Cu in a plasmonic Cu–Ag alloy decorated SiO2@S-doped C3N4 core–shell nanostructured photocatalyst towards enhanced visible light activity. Nanoscale Advances, 0, , .	2.2	8
416	Studies on Indian Ocean Manganese Nodules. Journal of Colloid and Interface Science, 1996, 183, 374-379.	5.0	7
417	Liquid phase mononitration of chlorobenzene over WOx/ZrO2: A study of catalyst and reaction parameters. Journal of Molecular Catalysis A, 2006, 260, 35-42.	4.8	7
418	Effects of preparation methods on gold/titania catalysts for CO oxidation. Journal of Molecular Catalysis A, 2008, 288, 125-130.	4.8	7
419	La ₂ Ti ₂ O ₇ As Nanometric Electrode Material: An Emerging Candidate For Supercapacitor Performance. ChemistrySelect, 2019, 4, 12037-12042.	0.7	7
420	Designing of a novel p-MoS2@n-ZnIn2S4 heterojunction based semiconducting photocatalyst towards photocatalytic HER. Materials Today: Proceedings, 2021, 35, 268-274.	0.9	7
421	Tailoring the fusion effect of phase-engineered 1T/2H-MoS ₂ towards photocatalytic hydrogen evolution. New Journal of Chemistry, 2022, 46, 14922-14932.	1.4	7
422	Studies on Indian Ocean Manganese Nodules. Journal of Colloid and Interface Science, 1998, 200, 249-255.	5.0	6
423	Effect of calcination temperature on Indian Ocean manganese nodules. Mössbauer, XRD, FT-IR and TG-DTA studies. Thermochimica Acta, 1999, 325, 69-76.	1.2	6
424	Facile Fabrication of Organicâ€Inorganic Hybrid Material Based on Wellâ€Dispersed AuNPs on Organoâ€Functionalised Znâ€Alâ€Layered Double Hydroxides for Hydroamination of 1â€Hexene. ChemistrySelect, 2018, 3, 3092-3100.	0.7	6
425	Facile synthesis of fullerene modified ZnFe2O4 composites towards photocatalytic H2 evolution under visible light irradiation. Materials Today: Proceedings, 2021, 35, 203-206.	0.9	6
426	Oxidative coupling of methane over Bi2O3â^'P2O5â^'K2O/Sm2O3. Reaction Kinetics and Catalysis Letters, 1991, 44, 103-108.	0.6	5
427	Studies on Indian Ocean Manganese Nodules. Journal of Colloid and Interface Science, 1998, 197, 236-241.	5.0	5
428	Synthesis and Surface Properties of Silica Spheres with Core Shell Structure by One Convenient Method. Research Letters in Materials Science, 2009, 2009, 1-5.	0.2	5
429	Comparison of NiFe-LDH based heterostructure material towards photocatalytic rhodamine B and phenol degradation with water splitting reactions. Materials Today: Proceedings, 2021, 35, 243-246.	0.9	5
430	Noble metal loaded ZnCr-LDH based hybrid material for Suzuki coupling reactions: A comparison study on heterogeneous catalysis with photo catalysis. Materials Today: Proceedings, 2021, 35, 229-232.	0.9	5
431	Biomimetic Synthesis of Silver Nanoparticles by Aqueous Extract of <l>Cinnamomum</l> <l>tamala</l> Leaves: Optimization of Process Variables. Nanoscience and Nanotechnology Letters, 2014, 6, 409-414.	0.4	5
432	Importance of specific surface area and basic sites of the catalyst in oxidative coupling of CH4 over LiO/MgO catalysts prepared by precipitation methods. Reaction Kinetics and Catalysis Letters, 1991, 44, 95-101.	0.6	4

#	Article	IF	CITATIONS
433	Studies on Indian Ocean Manganese Nodules. Journal of Colloid and Interface Science, 1997, 187, 453-458.	5.0	4
434	Studies on Indian Ocean Manganese Nodules. Journal of Colloid and Interface Science, 1998, 202, 313-317.	5.0	4
435	Solar Fuels from CO ₂ Photoreduction over Nano-Structured Catalysts. Materials Science Forum, 0, 855, 1-19.	0.3	4
436	Nanocomposites of g-C3N4 with Carbonaceous ï€-conjugated/Polymeric Materials Towards Visible Light-Induced Photocatalysts. Springer Series on Polymer and Composite Materials, 2017, , 251-294.	0.5	4
437	Studies ofÎ ² -FeOOH. Chemical composition, microstructure and other characteristics of some synthetic agakaneite samples. Journal of Materials Science Letters, 1987, 6, 1476-1478.	0.5	3
438	Effect of Anions (Cl ^{â^'} , SO ^{2â^'} ₄) on the Interfacial Properties of Akaganeite (β-FeOOH) in Aqueous Electrolyte Solutions. Adsorption Science and Technology, 1988, 5, 257-279.	1.5	3
439	Studies on Idian ocean manganese nodules, VII. Effect of Î ³ -irradiation on the physico-chemical properties and catalytic activity of polymetallic nodules. Reaction Kinetics and Catalysis Letters, 1997, 62, 191-199.	0.6	3
440	Photo-oxidation of phenol over titania pillared zirconium phosphate and titanium phosphate. Journal of Molecular Catalysis A, 2005, , .	4.8	3
441	Studies on manganese nodule leached residue. Journal of Colloid and Interface Science, 2006, 294, 117-121.	5.0	3
442	Titanium-Based Mixed Metal Oxide Nanocomposites for Visible Light-Induced Photocatalysis. Springer Series on Polymer and Composite Materials, 2017, , 295-331.	0.5	3
443	Construction of surfactant/polymer/copolymer-templated mesoporous reduced graphene oxide nanoparticles for adsorption applications. Graphene Technology, 2019, 4, 53-59.	1.9	3
444	Facile Synthesis and Synergetic Interaction of VPO/ \hat{l}^2 -SiC Composites toward Solvent-Free Oxidation of Methanol to Formaldehyde. ACS Omega, 2020, 5, 22808-22815.	1.6	3
445	Efficient perovskite titanate photocatalysts for oxygen evolution reactions. Materials Today: Proceedings, 2021, 35, 133-136.	0.9	3
446	Zr-based MOF: An enhanced photocatalytic application towards H2 evolution by consequence of functional group and LSPR effect. Materials Today: Proceedings, 2021, 35, 198-202.	0.9	3
447	An amine functionalized ZnCr LDH/MCM-41 nanocomposite as efficient visible light induced photocatalyst for Cr(VI) reduction. Materials Today: Proceedings, 2021, 35, 252-257.	0.9	3
448	Photo-catalytic H2 evolution over Au modified mesoporous g-C3N4. Materials Today: Proceedings, 2021, 35, 247-251.	0.9	3
449	Studies on the effects of CO2 and CO on n-butane isomerisation activity over sulfated zirconia. Journal of Molecular Catalysis A, 2002, 185, 237-248.	4.8	2
450	Studies on sulphatization—l. Sulphatization of manganese ore with pyrite. Journal of Chemical Technology and Biotechnology, 1988, 41, 223-230.	1.6	2

#	Article	IF	CITATIONS
451	Fabrication of VMn@mesoporous silica for epoxidation of cyclohexene. Journal of Porous Materials, 2012, 19, 225-232.	1.3	2
452	Cs salt of tungstophosphoric acid-promoted zirconium titanium phosphate solid acid catalyst: An active catalyst for the synthesis of bisphenols. Journal of Chemical Sciences, 2014, 126, 455-465.	0.7	2
453	Catalytic activity of vanadium-substituted molybdophosphoric acid supported on titania for the vapor-phase synthesis of isophthalonitrile. Inorganic and Nano-Metal Chemistry, 2017, 47, 1429-1435.	0.9	2
454	Adsorption study of hexavalent chromium by porous and non-porous ZnFe2O4. Materials Today: Proceedings, 2021, 35, 289-293.	0.9	2
455	A comparison study between novel ternary retrieval NiFe2O4@P-doped g-C3N4 and Fe3O4@P-doped g-C3N4 nanocomposite in the field of photocatalysis, H2 energy production and super capacitive property. Materials Today: Proceedings, 2021, 35, 281-288.	0.9	2
456	Studies on Indian Ocean Manganese Nodules. Journal of Colloid and Interface Science, 1999, 210, 130-133.	5.0	1
457	Fabrication of Mesoporous MnO2-MCM-41 Composite: A Promising Material for Photocatalytic Degradation of Organic Dyes Under Visible Light. Advanced Science Letters, 2014, 20, 579-583.	0.2	1
458	Photo-/Electro-catalytic Applications of Visible Light-Responsive Porous Graphitic Carbon Nitride Toward Environmental Remediation and Solar Energy Conversion. Environmental Chemistry for A Sustainable World, 2020, , 211-246.	0.3	1
459	Homogeneous precipitation of molybdenum oxinate and its estimation in a multicomponent system Bunseki Kagaku, 1984, 33, E481-E485.	0.1	0
460	Catalytic activity of transition metal mixed amorphous aluminium phosphate towards alcohol conversion reactions Studies in Surface Science and Catalysis, 1998, , 963-973.	1.5	0
461	Characterization of Nano-Crystalline Nickel Supported Zirconia and its Catalytic Activity of Hydrogenation of Nitrophenol. , 2011, , .		0
462	Corrigendum to "Efficient hydrogen production by composite photocatalyst CdS–ZnS/zirconium–titanium phosphate (ZTP) under visible light illumination―[International Journal of Hydrogen Energy, 36 (2011) 13452–13460]. International Journal of Hydrogen Energy, 2012, 37, 6118.	3.8	0
463	Probing bifunctional nature of aluminium promoted vanadium phosphate: a versatile catalyst for oxidation and esterification. International Journal of Advances in Engineering Sciences and Applied Mathematics, 2013, 5, 219-223.	0.7	0
464	Transition Metal-Substituted Salt of Tungsten-Based Polyoxometalate-Supported Mesoporous Silica as a Catalyst for Organic Transformation Reactions. , 2013, , 57-90.		0
465	Quantification of boron contents in BN/BCN composites by prompt gamma-ray neutron activation analysis utilizing thermal neutron beam at Dhruva reactor. Journal of Radioanalytical and Nuclear Chemistry, 2020, 325, 977-982.	0.7	0
466	CdS QDs sensitized various Bi based semiconductors: A comparison study on clean energy production under visible light irradiation. Materials Today: Proceedings, 2021, 35, 216-220.	0.9	0
467	Visible light responsive 2DCeO2-CdSQDs binary hybrid towards photocatalytic degradation of phenol. Materials Today: Proceedings, 2021, 35, 263-267.	0.9	0
468	Design of Nano CuO Modified Ordered Mesoporous Carbon for Single Step Oxidation of Benzene. Advanced Science Letters, 2014, 20, 650-653.	0.2	0

#	Article	IF	CITATIONS
469	Adsorptive-Photo-Reduction of Aqueous Cr(VI) lons by TiO ₂ @MCM-41 Under Visible Light. Advanced Science Letters, 2016, 22, 281-287.	0.2	0